

North-West road bypass of Merano - South Tyrol - Italy

G. Barovero

P.A.C. S.p.A, Capo di Ponte, Brescia, Italy

M. Moja, E.M. Pizzarotti & F. Prati

Pro Iter S.r.l., Milan, Italy

J. Strimmer

Autonomous Province of Bolzano, South Tyrol, Italy

ABSTRACT: The project consists of a 2.200 m long-tunnel, composed of a section in loose ground for about half of its total length and a section in metamorphic rock for the other half. The peculiarity of the portion in loose ground, on which this paper is focused, is that it crosses the town with shallow overburdens, about 10 m at most, running along or under numerous buildings. The rocky part, characterized by higher overburden, up to 100 m approximately, presents an underground roundabout with an overall diameter of 42 m, consisting of a toroidal tunnel with a central rock pillar of 8 m of diameter, for the connection with the future underground parking of Monte San Benedetto.

1 INTRODUCTION

The North-West Ring Road of Merano, Lot 2, is a project of the Autonomous Province of Bolzano (APB), that completes the fast-flowing access and exit road from the city center and connects the existing Bolzano-Merano Highway, to the West, and the Val Passiria route, to the East, continuing the penetration axis of Lot 1, already completed in the past years.

The Detailed Design was made by the design team composed of Dr. Eng. A. Gretzer, Dr. Eng. K. Bergmeister, Dr. Eng. M. Ebner and Dr. Eng. W. Weis.

The contract for the construction of the works, for an amount of about 100 M €, was awarded to the consortium San Benedetto - Merano Scarl, made up of the mandatory Carron Bau S.r.l. and Mair Josef & Co S.a.s., Di Vincenzo Dino & Co S.p.A. and PAC S.p.A., which has entrusted the consultancy for the For Construction Design to the engineering company Pro Iter S.r.l.

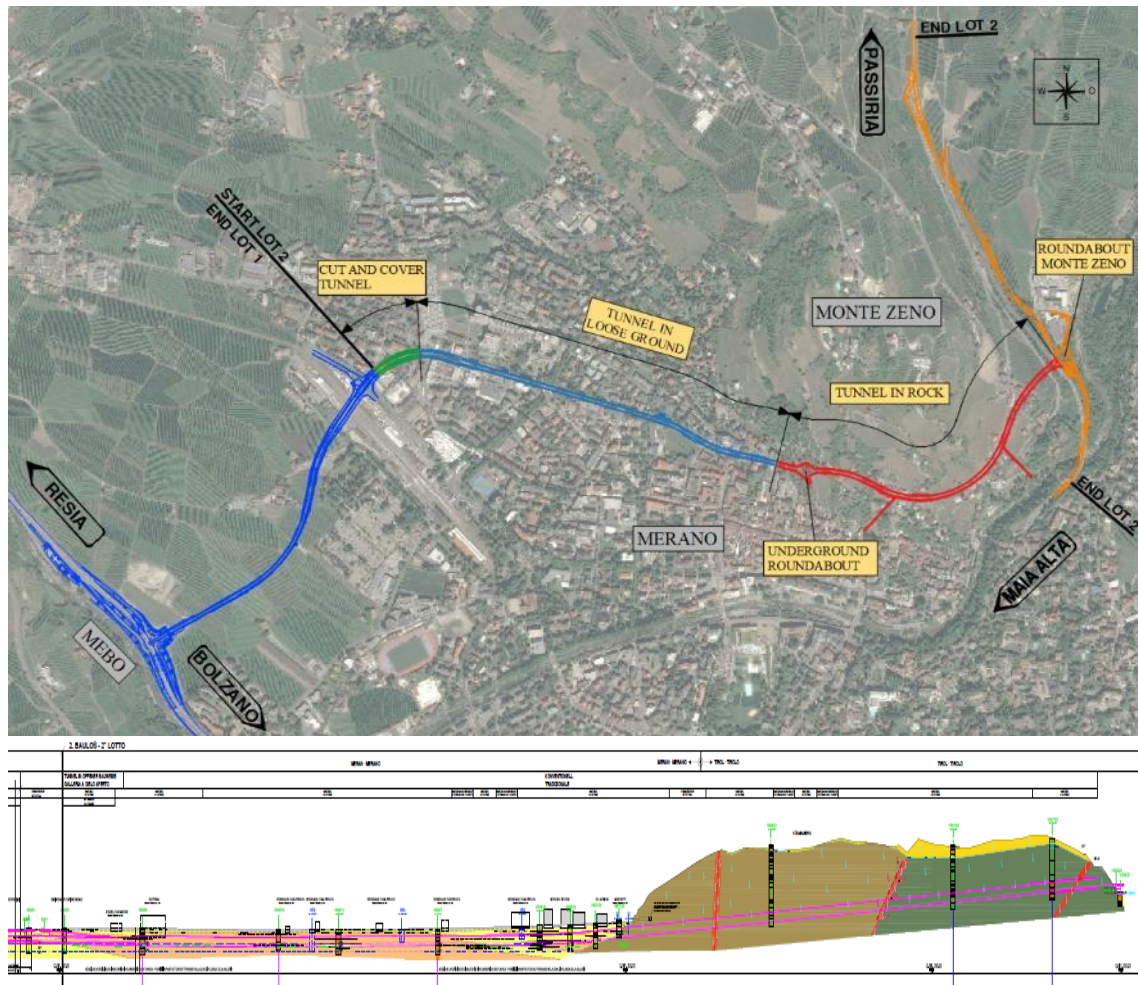
In this paper, after a brief description of the entire project, the choices made for the excavation of the natural tunnel under shallow overburden in loose ground are described.

2 THE PROJECT

The road layout of Lot 2 starts in the North-West part of Merano, in continuity with Lot 1, which has already been completed and is currently in operation, runs eastwards under the city and then connects to the existing road system of Passiria Valley.

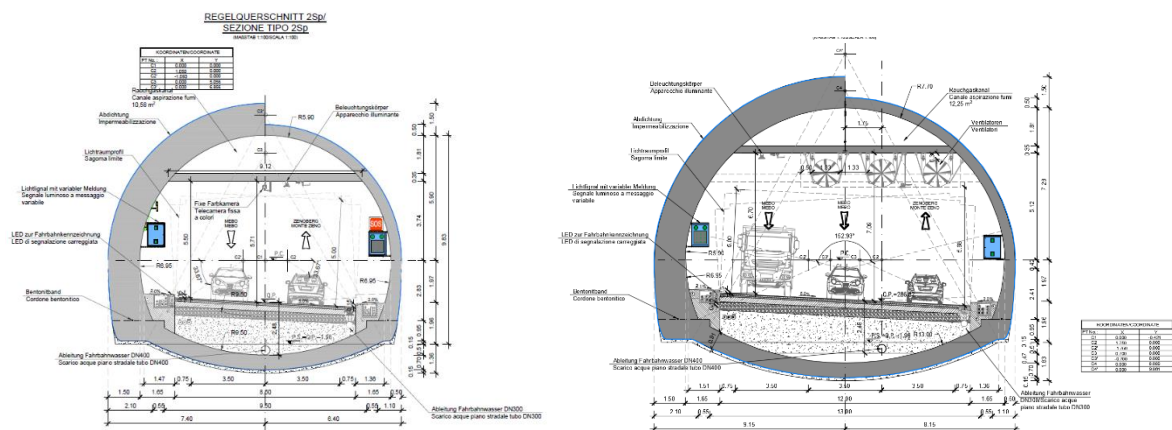
Except for the open-air sections to the East, Lot 2 mainly consists of a single tunnel with a total length of about 2200 m, which can be divided into two parts: an initial section of Cut&Cover tunnel (L=136 m, Pizzarotti E.M. et al., 2022.), connected to Lot 1 and the surface roads, and a subsequent section of conventional underground excavation (L=2064 m).

The latter, approximately for the first km, crosses the city of Merano and is characterized by the presence of loose ground and shallow overburdens; moving eastward, the tunnel crosses the metamorphic rock formations of Mount San Benedetto, with overburdens up to about 100 m (Figure 1).



The loose ground is mostly gravels and sandy gravels, with pebbles and frequent boulders, generally less than 1 m³, having the following average geotechnical parameters: $\gamma = 22 \text{ kN/m}^3$, $\phi' = 35^\circ$, $c' = 0 \text{ kPa}$ and $E = 120 \text{ MPa}$.

The rocky part of the route crosses the Periadriatic lineament, here called the Merano-Mules fault, which separates the South Alpine unit of Brixen, consisting of cornubianitic phyllites, from the Austroalpine Marling formation, with predominantly gneisses and mica schists often cataclastic.



of the analyses carried out (see in the following), the heaviest section 2Sp_6 was foreseen in the stretch where the tunnel underpasses some buildings (foundations vertical distance from the tunnel crown less up to 6 m), the intermediate section 2Sp_9 (Figure 4) in presence of buildings at a horizontal distance from the tunnel axis between 6 m and 15 m, while the lightest section 2Sp_12 was foreseen in green-field condition or where the buildings have a horizontal distance from the tunnel axis > 15 m.

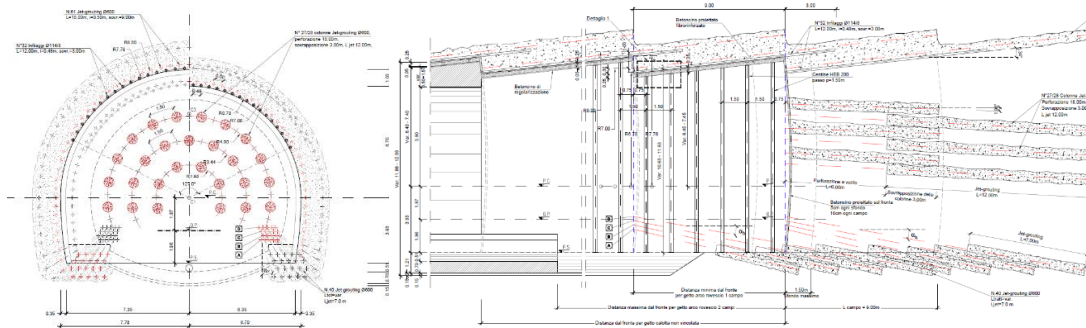


Figure 4. Excavation support for Section 2Sp_9

The same injections and supports described above were applied for the excavation of the lay-bays Pb, even if, considering the higher excavation dimensions of the section (on average 18 m width and 14 m height versus 14.5 m width and 12.5 m height for the 2Sp section), only rounds of excavation of 6 m and 9 m were foreseen.

A different approach has been adopted for the excavation of the largest section 4Sp (Figure 5), that reaches an excavation width of about 21 m and a height of about 13.5 m, for which a sawtooth section, also given the shallow overburden of approximately 6 m, is not applicable. In this case, the design foresees the excavation of a pilot tunnel (2Sp*), with dimensions and supports similar to section 2Sp, the execution of radial cement-bentonite mix injections 4.5 m thick via PVC tubes with valves (3 valves/m) from the pilot tunnel to the boundary of the section and the successive enlargement with the installation of the primary lining (5+25 fiber sprayed concrete reinforced with steel ribs HEB200 every 0.75 m).

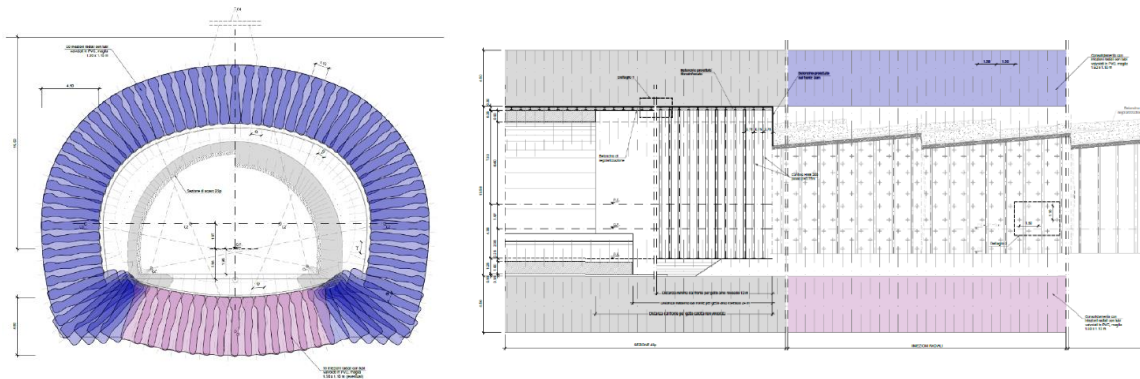


Figure 5. Excavation support for Section 4Sp

For the design of the tunnel in loose ground and under low overburden, 3D FDM step-by-step analyses with the software Flac3D were carried out to simulate all the excavation phases with the aim of: 1) studying the stability of the excavation face; 2) assessing a reliable de-confinement law (relation between displacements and the distance from the face, to be used in the successive and more specific 2D analyses); 3) obtaining an evaluation of the trend of the longitudinal settlements on surface along the axis.

The excavation section considered in the 3D analyses is 2Sp, the most present along the route. For the sake of simplicity, the mean section with a cylindrical shape has been modelled.

The step-by-step analyses simulate the progressive advancement of the excavation with the execution of all the stabilization measures of the tunnel as well as the primary lining and the

successive casting of the final lining (Figure 6). In particular, the various measures have been modelled as follow:

- The umbrella fields on the contour of the cavity using uniaxial pile element capable of supporting axial, shear and bending moment actions.
- The jet-grouting injections on the contour of the cavity and on the excavation face through the increment of the cohesion property of the ground injected.
- The primary lining and the final lining (invert and crown) by 3D shell elements.

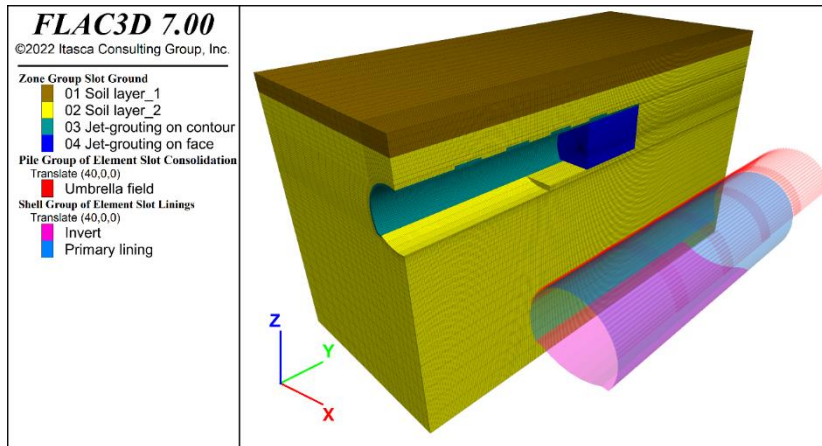


Figure 6. Step by Step 3D analysis – Section 2Sp_12 – Soil group and structural elements

The analyses of excavation face stability (Figure 7) have been performed applying a reduction to the strength parameters of the soil through a coefficient (Factor of Safety FoS) following the Italian standards. Those analyses allow to size the injections intensity necessary to ensure the safety of the excavation face.

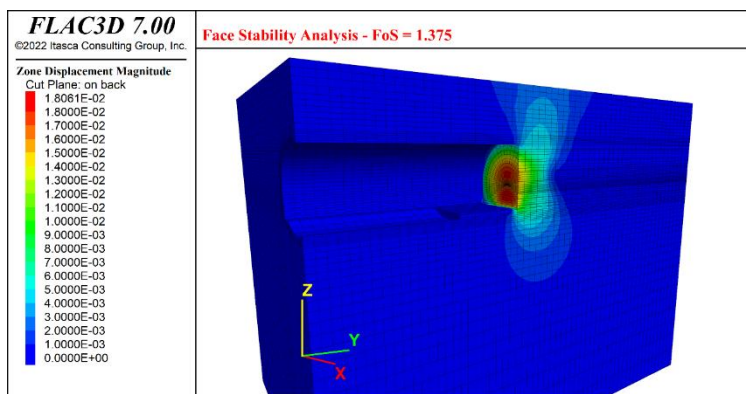


Figure 7. Face Stability Analysis results – Section 2Sp_12 – FoS = 1.375 – Displacement magnitude plot

Successive 2D FDM analyses with Flac2D have been performed to study:

- The various configurations of the tunnel related to three different conditions: the absence of buildings (green field), the presence of buildings at a minimum horizontal distance from the tunnel axis equal to 6 m and the presence of building above the tunnel (Figure 8).
- The other sections present in the project with a dimension greater than section 2Sp (Pb,4Sp).
- The effect of specific load conditions, such as the seismic load, the water pressure, the weight loads due to the presence of the ventilation duct slab and the load dissymmetry due to the possible future side trenching.

The 2D analyses allowed the sizing of the primary and final linings and the evaluation of the surface subsidence in different boundary conditions (Figure 9).

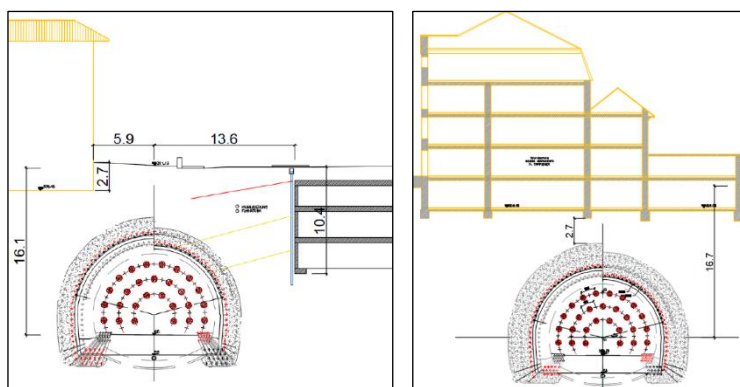


Figure 8. Passage of the section 2Sp_9 near the building (on the left) and passage of the section 2Sp_6 under the buildings (on the right)

The evaluation of the subsidence with the 2D analyses has been integrated with analytical formulation based on Peck (1969), O'Reilly and New (1991) and Burland (1995), describing the settlements trend with a Gaussian curve, to perform sensitive analyses to evaluate the maximum possible subsidence and distortion below the existing buildings. The keys parameters in the analytical model, i.e., the Volume Loss V_L and the coefficient k , were, at first, estimated according to the results of the 2D analyses. Successively, these parameters have been varied with the aim of studying more conservative scenarios (Figure 10).

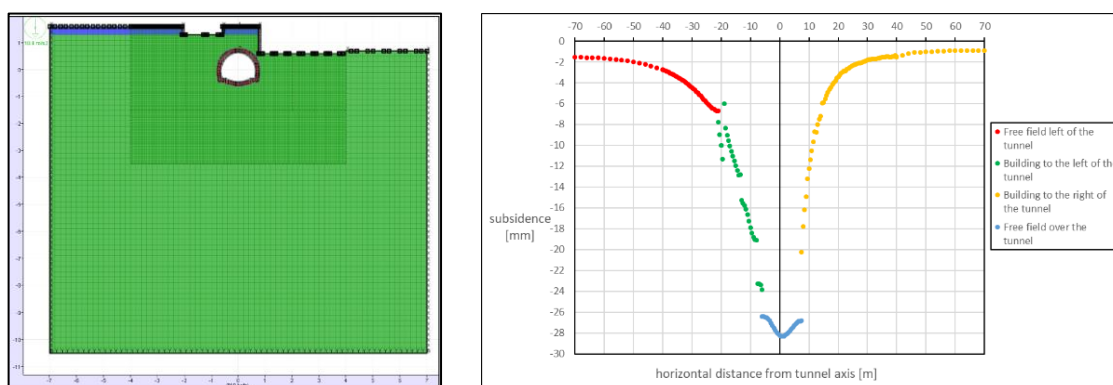


Figure 9. 2D analysis for the evaluation of the subsidence on surface and below the buildings (on the left); Development of the subsidence (on the right)

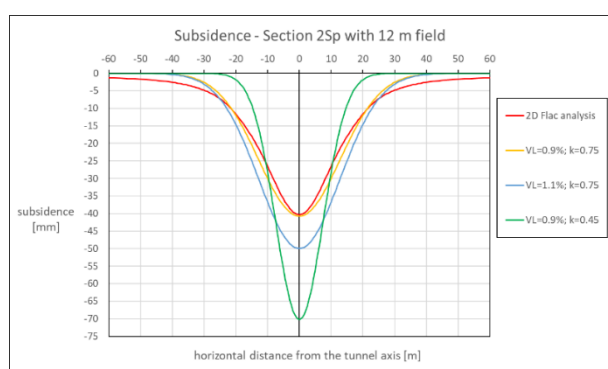


Figure 10. Comparison of subsidence curve: 2D numerical analysis (red), analytical model (yellow) and analytical model under conservative scenarios with increasing Volume Loss (blue) and decreasing of k coefficient (green)

Based on the results of these conservative analyses, the Attention and Alarm threshold values regarding the subsidence and the distortion on the free-field and below the existing buildings were defined, to limit the level of buildings damage within acceptable values (risk category n. 2 in Rankin classification “light damage level – cracks easily removed by painting”). From Table 1 and Table 2, it is possible to notice that the threshold values are never exceeded by the results of

numerical analyses and are reached only considering the conservative analytical analysis ($V_L = 1.1\%$ for the Attention value and $k = 0.45$ for the Alarm value).

Table 1. Maximum subsidence values on the surface from analytical and numerical analyses and relative Attention and Alarm thresholds values

Maximum subsidence values (Smax)				
Reference Section	Smax analytical method [mm]	Smax numerical analysis [mm]	Smax threshold value of Attention [mm]	Smax threshold value of Alarm [mm]
2Sp_6 (VL=0.5%)	23	24	50	80
2Sp_9 (VL=0.7%)	33	26		
2Sp_12 (VL=0.9%)	42	40		
Pb_6 (VL=0.5%)	33	33	50	80
Pb_9 (VL=0.7%)	47	38		
2Sp*_9 (VL=0.7%)	33	26		
2Sp*_12 (VL=0.9%)	42	40	50	80
4Sp	-	97	100	130

Table 2. Maximum subsidence and distortion under buildings from analytical and numerical analyses and relative Attention and Alarm thresholds values

Reference Section	Maximum subsidence values under buildings (Smax)				Maximum distortion under buildings (Dmax)			
	Smax analytical analysis [mm]	Smax numerical analysis [mm]	Smax threshold value of Attention [mm]	Smax threshold value of Alarm [mm]	Dmax analytical analysis [-]	Dmax numerical analysis [-]	Dmax threshold value of Attention [mm]	Dmax threshold value of Alarm [mm]
2Sp_6 (VL=0.5%)	23	30	30	50	1/872	1/606	1/350	1/200
2Sp_9 (VL=0.7%)	29	24			1/623	1/432		
2Sp_12 (VL=0.9%)	20	-			1/510	-		
Pb_6 (VL=0.5%)	30	24			1/615	1/533		
Pb_9 (VL=0.7%)	22	-			1/462	-		
2Sp*_9 (VL=0.7%)	29	24			1/623	1/432		
2Sp*_12 (VL=0.9%)	20	-			1/510	-		
4Sp	-	35			-	1/367		

The threshold values were defined differently in relation to the relative position of the monitoring section respect to the actual location of the excavation face.

In particular, for monitoring sections beyond the excavation face, the threshold values have been set equal to the 30% of the respective values far behind the excavation face, as shown in Table 3, according to the longitudinal trend of the surface subsidence provided by both the 3D analyses and the literature (Attewell e Hurrell (1985) and Ribacchi (1993)).

Table 3. Attention and Alarm thresholds values beyond the excavation face

Attention and alarm thresholds values - Maximum subsidence (Smax) and distortion (Dmax) Monitoring section on surface NOT yet undercut by the tunnel excavation						
Reference Section	Smax free field [mm]		Smax under buildings [mm]		Dmax under buildings [-]	
	Attention	Alarm	Attention	Alarm	Attention	Alarm
2Sp; Pb; 2Sp*	15	25	10	15	1/1000	1/600
4Sp	65	95				

Note: the threshold values for section 4Sp have been obtained considering the 100% of the section 2Sp* threshold and 30% of section 4Sp (enlarged excavation) incremental threshold.

To check the correctness of the design predictions, continuous surface monitoring was planned, essentially based on subsidence control, using total stations able to detect hourly the subsidence on specific cross-sections, spaced approximately 10 metres apart. Each section consists of 5-6 optical targets or topographic prisms (Figure 12).

4 CONCLUSION

The excavation in the loose ground started from the West side with section 2Sp* - after the initial section of Cut&Cover tunnel - and from the East side with section 2Sp - after the completion of the rocky part and the overcoming of the contact between loose ground and rock - reaching respectively, at the date of the present paper, for a length of about 130 m and a length of approximately 55 m (Figure 11), with advancement rates close to one meter per day.



Figure 11. Excavation face in loose material (from West portal – section 2Sp* on the left) and in proximity to the passage from the rock to the loose material from the East portal (Section 2Sp on the right)

During the excavation of the first portions of the tunnel, the recorded subsidence has been less than or, in the worst conditions, similar to the value predicted in the design phase (Figure 12). The back-analysis of the data acquired during this phase suggested to modify the heaviest section foreseen in the design to underpass the buildings (2Sp_6) with a new section similar to the section 2Sp_9 but with the following enhancements: 1 – Reinforcing the jet-grouting column on the boundary with steel tubes; 2 – Increasing the number of the jet-grouting columns on the front, particularly in the upper part of the section. Excavating with a longer field (9 m instead of 6 m) has the beneficial effect of reducing the inclination of the treatments on the boundary and consequently the distance of the jet-grouting injections from the foundations of the buildings.

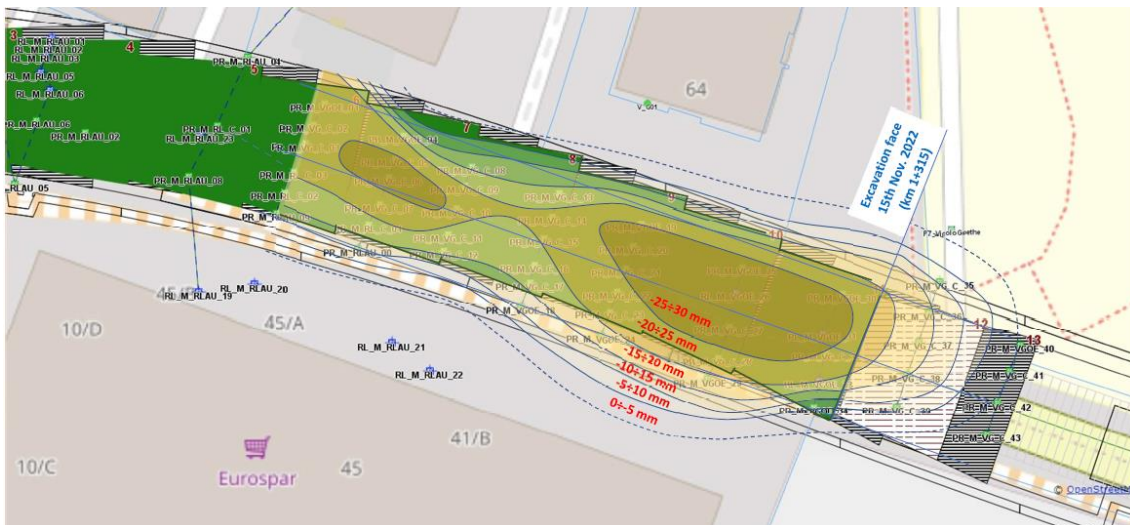


Figure 12. Plan view of the continuous surface monitoring and subsidence (West side)

REFERENCES

- Attewell P.B., Hurrell M.R., 1985. Settlement development caused by tunnelling in soil. *Ground Engineering*: 17-20.
- Burland J.B., 1995. Assessment of risk damage to buildings due to tunnelling and excavation. *Proceedings of the 1st International Conference in Earthquake Engineering*: 1189-1201. Tokyo: IS.
- O'Reilly M.P., New B.M., 1982. Settlements above tunnels in the United Kingdom – their magnitude and prediction, *Tunnelling* 82: 310-329. London: IMM.
- Peck R.B., 1969. Deep excavation and tunnelling in soft ground. *Proc. 7th International Conference Soil Mechanics and Foundation Engineering - State of the Art Volume*: 225-290. Mexico City.
- Pizzarotti E.M., Donelli M., Moja M., Prati F., Readaelli P., Regondi L., Strimmer J., 2022 North-West Ring Road of Merano - 2nd Lot: Cut&Cover Tunnel. *Italian Concrete Conference* - Naples, October 2022.